Analysis of a single-phase capacitor induction motor operating at two power line frequencies

ALEKSANDER LEICHT, KRZYSZTOF MAKOWSKI

Institute of Electrical Machines, Drives and Measurements, Wroclaw University of Technology
Smoluchowskiego 19, 50-372 Wroclaw 51, Poland
e-mail: {aleksander.leicht / krzysztof.makowski}@pwr.wroc.pl

Abstract: The paper presents a modelling mathematical tool for prediction of dynamic and steady-states operation of the single-phase capacitor induction motor for different values of the capacitor capacitance and different frequency of voltage supply at no-load and rated load conditions. Developed mathematical model of the capacitor induction motor was implemented for calculation using Matlab/Simulink software. Presented simulation results may be utilized to achieve better starting quality of single-phase capacitor induction motors.

Key words: induction motors, single-phase, capacitor motors, circuit modelling, simulation, starting quality factor

1. Introduction

Single-phase capacitor induction motors are commonly used as a drive for low-power fans, pumps and compressors [1]. Generally, they are induction machines of the symmetrical rotor cage and two non-symmetrical stator windings (the main winding and auxiliary winding with starting or running capacitor), supplied with the same sinusoidal voltage source. In modelling performance characteristics of the induction motors circuit models of lumped parameters are still often used due to their simplicity and fast computation. Many papers dealing with analysis of single-phase capacitor induction motors have been published so far and some of them are cited in Reference. In [4] Authors used universal machine model as a part of electromagnetic transients power system commercial package (EMTP) for modelling and analysis of the single-phase induction motor with two capacitors (starting and running) in auxiliary stator winding. Employing the *dq* model of the motor they showed simulation waveforms of electro-magnetic torque and stator currents in case of the capacitor–start and capacitor–run operation with observation of the effects of the capacitor on torque pulsation. Obtained by the EMTP program simulation results were in good agreement with laboratory testing results. In the

paper [5] a dynamic model of the single-phase induction motor at capacitor-start and capacitor-run mode was analysed using PSPICE software package. Using this software the motor operation was described by a set of time-varying differential equations and comparison of motor waveforms between simulated and experimental ones was satisfactory. The Authors reported a more accurate and reasonable results as compared with those obtained by the EMTP program. Authors of the paper [6] applied generalized averaging method (phasor-dynamic modelling technique) to the conventional model of a single-phase induction motor. They obtained outstanding agreements in plots of instantaneous torque and rotational speed from standard model and theirs envelopes from phasor-dynamic model. The method is proposed to be used in high-performance control algorithms. These models may be fully useful for selection of capacitance of starting/running capacitor and for searching of better operation parameters or showing direction of the searching in design optimization.

In the paper a mathematical model of the single-phase capacitor induction motor in the stationary *dq* system is described and developed for simulation start-up of the motor at no-load and application of nominal load torque after starting from no-load operation. The general model and parameters of the capacitor induction motor in the *dq* system for steady-state operation was described in [7, 9, 10]. At first approximation of the mathematical models linearity of magnetic circuit is assumed and slotting of the stator and rotor are neglected [2-3]. Basic experimental verification of the model which was used in the analysis was presented in the paper [8] and showed correctness of the analytical model. The present paper deals with simulations of dynamic and steady-state characteristics of a tested capacitor induction motor for different values of capacitor capacitance placed in the auxiliary stator winding supplies from sinusoidal voltage source of 230 V at frequency of 50 and 60 Hz.

2. Description of a tested motor

As an object of research is the low power, single-phase capacitor induction motor. Its cross-section and the *dq* model are presented in Figure 1. The motor has two stator windings: the main (M) and the auxiliary (A) winding. Their magnetic axes are displaced by 90°. The running capacitor is placed in series with the auxiliary winding. The rotor has squirrel cage of 11 bars, that are distributed uniformly along rotor's circumference. Table 1 lists the ratings and structural data of the tested motor.

3. Simulation *dq* models of the motor

Since the axes of both stator windings are orthogonal, the *dq* axes of the model may be aligned with axes of the windings, as illustrated in Figure 1. The squirrel cage rotor may be represented by a pair of symmetrical, short-circuited coils.

Table 1. Ratings and data of the tested capacitor induction motor

Rated power	0.09 kW
Rated voltage	230 V
Rated current	0.9 A
Rated speed	2840 rev/min
Efficiency	0.55
Power factor	0.9
Frequency	50 Hz
Torque ratio	1.5
Number of stator windings	2
Running capacitor capacitance	3 μF
Connection of stator windings	parallel
Number of poles: main/auxiliary winding	2/2
Winding layout: main/auxiliary winding	single layer
Rotor winding	squirrel cage
Number of slots: stator/rotor	18/11
Lamination material - generator sheet	M 600-50 A
Laminated core length	32 mm
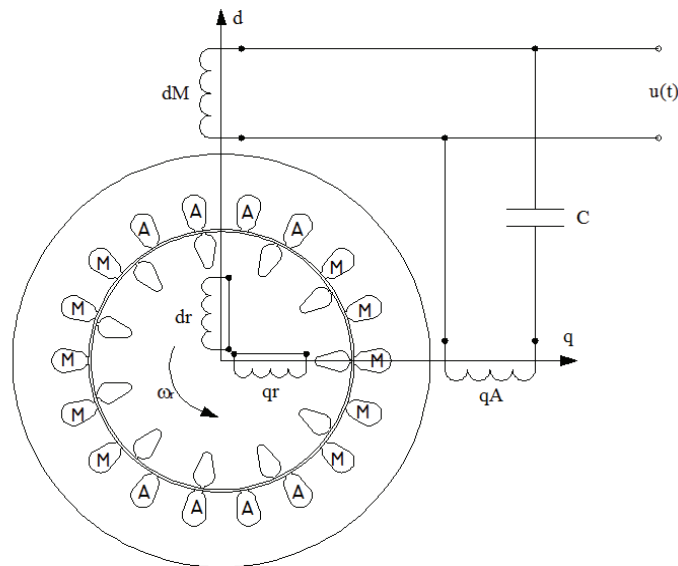
Fig. 1. Cross section view and the *dq* model of tested capacitor induction motor

The circuit model of the capacitor induction motor can be described by differential equations written as follows:

$$\frac{di_{dM}}{dt} = \frac{R_s L'_{rr}}{L_\Sigma} i_{dM} + \frac{L_m^2}{L_\Sigma} \omega_r i_{qA} - \frac{L_m L'_{rr}}{L_\Sigma} i'_{dr} + \frac{L_m L'_{rr}}{L_\Sigma} \omega_r i'_{qr} - \frac{L'_{rr}}{L_\Sigma} u_{dM} + \frac{L_m}{L_\Sigma} u'_{dr}$$

$$\frac{di_{qA}}{dt} = -\frac{L_m^2}{L_\Sigma} \omega_r i_{dM} + \frac{R_s L'_{rr}}{L_\Sigma} i_{qA} - \frac{L_m L'_{rr}}{L_\Sigma} \omega_r i'_{dr} - \frac{L_m L'_{rr}}{L_\Sigma} i'_{qr} - \frac{L'_{rr}}{L_\Sigma} u_{qA} + \frac{L_m}{L_\Sigma} u'_{qr} + \frac{L'_{rr}}{L_\Sigma} u_{qC}$$

$$\frac{di'_{dr}}{dt} = -\frac{R_s L_m}{L_\Sigma} i_{dM} - \frac{L_m L_{ss}}{L_\Sigma} \omega_r i_{qA} + \frac{R'_r L_{ss}}{L_\Sigma} i'_{dr} - \frac{L_m^2}{L_\Sigma} \omega_r i'_{qr} - \frac{L_{ss}}{L_\Sigma} u'_{dr} + \frac{L_m}{L_\Sigma} u_{dM} \qquad (1)$$

$$\frac{di'_{qr}}{dt} = \frac{L_m L_{ss}}{L_\Sigma} \omega_r i_{dM} - \frac{R_s L_m}{L_\Sigma} i_{qA} + \frac{L_m^2}{L_\Sigma} \omega_r i'_{dr} + \frac{R'_r L_{ss}}{L_\Sigma} i'_{qr} + \frac{L_m}{L_\Sigma} u_{qA} - \frac{L_{ss}}{L_\Sigma} u'_{qr} - \frac{L_m}{L_\Sigma} u_{qC}$$

$$\frac{du_{qC}}{dt} = \frac{1}{C} i_{qA}$$

$$\frac{d\omega_r}{dt} = \frac{p^2}{J} L_m \left(i_{dM} i'_{qr} - i_{qA} i'_{dr} \right) - \frac{D_f}{J} \omega_r - \frac{p}{J} T_L,$$

where:

$$L_\Sigma = L_m^2 - L'_{rr} L_{ss}, \, R_s = R_M = R'_A, \, L_{ss} = L_{sM} = L'_{sA}$$

and i_{dM}, i_{qA} are the direct- and quadrature-components of stator currents, i_{dr}, i_{qr} are the direct- and quadrature-components of rotor currents, u_{dM}, u_{qA} are the direct- and quadrature-components of stator voltages, u_{dr}, u_{qr} are the direct- and quadrature-components of rotor voltages, u_{qC} is the voltage across the running capacitor, R_s is the resistance of stator windings, R_r is the resistance of rotor windings, L_{ss} is the self-inductance of stator windings, L_{rr} is the self-inductance of rotor windings, L_m is the magnetizing inductance, p is the number of pole-pairs, D_f is the viscous friction coefficient, J is the moment of inertia, T_L is the load torque, ω_r is the electrical angular velocity of the rotor.

Using the operator $s = d/dt$ and considering, that in squirrel-cage induction motor, the rotor windings are short-circuited (the both of the rotor voltages are equal to zero), and after some mathematical transformations, we obtain a set of the motor equations as follows:

$$i_{dM} = \frac{L_m}{L_\Sigma s - L'_{rr} R_s} \left[-R'_r i'_{dr} + \omega_r \left(L_m i_{qA} + L'_{rr} i'_{qr} \right) - \frac{L'_{rr}}{L_m} u_{dM} \right]$$

$$i_{qA} = \frac{L_m}{L_\Sigma s - L'_{rr} R_s} \left[-R'_r i'_{qr} - \omega_r \left(L_m i_{dM} + L'_{rr} i'_{dr} \right) - \frac{L'_{rr}}{L_m} u_{qA} \right]$$

$$i'_{dr} = \frac{1}{L_\Sigma s - L_{ss} R'_r} \left[-R_s L_m i_{dM} - \omega_r L_{ss} \left(L_m i_{qA} + L'_{rr} i'_{qr} \right) - L_m u_{dM} \right] \qquad (2)$$

$$i'_{qr} = \frac{1}{L_\Sigma s - L_{ss} R'_r} \left[-R_s L_m i_{qA} + \omega_r L_{ss} \left(L_m i_{dM} + L'_{rr} i'_{dr} \right) - L_m u_{qA} \right]$$

$$\omega_r = p \left(\frac{1}{Js + D_f} \right) \left[p L_m \left(i_{dM} i'_{qr} - i_{qA} i'_{dr} \right) - T_L \right],$$

where:

$$u_{qA} = -\left(u(t) - u_{qC}\right) = -u(t) + u_{qC}.$$

Steady-state circuit model allows for evaluation of electromagnetic torque and currents for given values of supply voltage and angular velocity. For steady-state operation, when assuming that the motor is supplied by a source of sinusoidal voltage, equations of the dq model of the motor may be written in complex form as follows:

$$
\begin{bmatrix}
\underline{U}_M \\
\underline{U}_A \\
0 \\
0 \\
\vdots \\
0 \\
0
\end{bmatrix}
=
\begin{bmatrix}
\underline{Z}_M & 0 & jX_{Mr1} & 0 & \cdots & jX_{Mrv} & 0 \\
0 & \underline{Z}_A - j/\omega C & 0 & jX_{Ar1} & \cdots & 0 & jX_{Arv} \\
jX_{Mr1} & kX_{Ar1} & \underline{Z}_{r1} & kX_{r1} & \cdots & 0 & 0 \\
-kX_{Mr1} & jX_{Ar1} & -kX_{r1} & \underline{Z}_{r1} & \cdots & 0 & 0 \\
\vdots & \vdots & \vdots & \vdots & \vdots & \vdots & \vdots \\
jX_{Mrv} & vkX_{Arv} & 0 & 0 & \cdots & \underline{Z}_{rv} & vkX_{rv} \\
-vkX_{Mrv} & jX_{Arv} & 0 & 0 & \cdots & -vkX_{rv} & \underline{Z}_{rv}
\end{bmatrix}
\cdot
\begin{bmatrix}
\underline{I}_M \\
\underline{I}_A \\
\underline{I}_{rd1} \\
\underline{I}_{rq1} \\
\vdots \\
\underline{I}_{rdv} \\
\underline{I}_{rqv}
\end{bmatrix},
\tag{3}
$$

where $\underline{Z}_M$, $\underline{Z}_A$ denote the impedances of the main and auxiliary windings, $\underline{Z}_{rv}$ is the impedance of the rotor winding for the v-th harmonic, C is the capacitance of the running capacitor, X_{Mrv}, X_{Arv} denote the mutual reactances between the main/auxiliary winding and the rotor cage for the v-th harmonic, X_{rv} is the reactance of the rotor winding for the v-th harmonic, $\underline{I}_M$, $\underline{I}_A$ are the currents of the stator windings, $\underline{I}_{rdv}$, $\underline{I}_{rqv}$ are the v-th harmonic rotor currents in the d and q axis, $\underline{U}_M$, $\underline{U}_A$ are voltages of the stator windings, p is the number of pole-pairs, s is the slip and $k = = (1 - s)/p$. Mean value of electromagnetic torque of the motor at steady-state may be expressed as:

$$T_{em} = \mathrm{Re}\left(p\,\mathbf{I}^{*T}\,\mathbf{G}\,\mathbf{I}\right),\tag{4}$$

where $\mathbf{I}$ is the vector of winding currents (the most right-hand side column matrix in equation (3)) and $\mathbf{G}$ is the matrix of rotational inductances, which takes the following form:

$$
\mathbf{G} =
\begin{bmatrix}
0 & 0 & 0 & 0 & \cdots & 0 & 0 \\
0 & 0 & 0 & 0 & \cdots & 0 & 0 \\
0 & L_{Ar1} & 0 & L_{rr1} & \cdots & 0 & 0 \\
-L_{Mr1} & 0 & -L_{rr1} & 0 & \cdots & 0 & 0 \\
\vdots & \vdots & \vdots & \vdots & \vdots & \vdots & \vdots \\
0 & vL_{Arv} & 0 & 0 & \cdots & 0 & vL_{rrv} \\
-vL_{Mrv} & 0 & 0 & 0 & \cdots & -vL_{rrv} & 0
\end{bmatrix},
\tag{5}
$$

where L_{Mrv}, L_{Arv} denote the mutual inductances between the main/auxiliary winding and the rotor cage for the v-th harmonic and L_{rrv} is the self inductance of the rotor cage for the v-th harmonic.

4. Dynamic characteristics of the motor

The simulation results in this section are obtained for a single-phase induction motor described in Paragraph 2., supplied with sinusoidal voltage of 230 V, 50 Hz and 60 Hz sources, at different capacitor capacitances, for two different cases:
- start-up of the motor with no-load ($T_L = 0$),
- start-up of the motor with no-load and applying the rated load ($T_L = T_N = 0.3$ Nm) after 0.7 s.

The simulations were performed at the assumption, that only moment of inertia of the motor $J = 0.00007$ kgm^2 and the viscous friction coefficient $D_f = 0.00005$ Nms were taken into account. In Figures 2-5 the motor starting waveforms obtained at no-load operation and for capacitor capacitance of 3 µF (capacitor chosen by the motor's manufacturer) are shown.
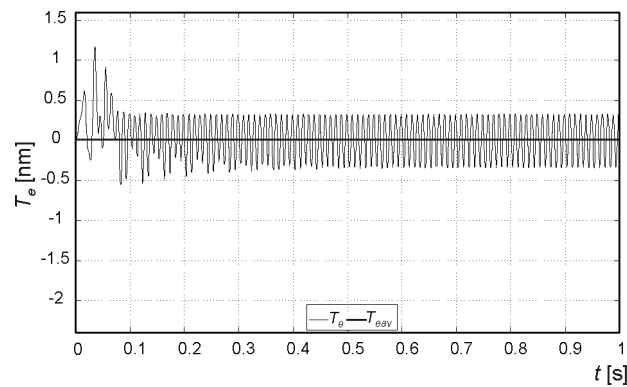
Fig. 2. The electromagnetic torque $T_e(t)$ at no-load for $C = 3$ µF, $f = 50$ Hz
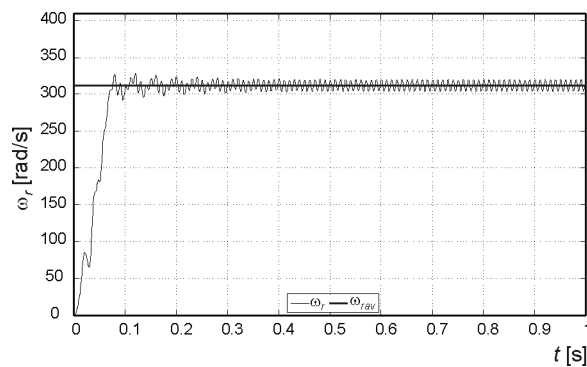
Fig. 3. The angular velocity $\omega_r(t)$ at no-load for $C = 3$ µF, $f = 50$ Hz

In all the figures, waveforms denoted with *av* present average values at steady-state.

It can be observed that the electromagnetic torque of single-phase capacitor induction motor has no constant value in steady-state. Showed torque oscillations (with a twice line frequency and amplitude $T_{em} = 0.31$ Nm) are caused by elliptical rotational field in the air-gap,
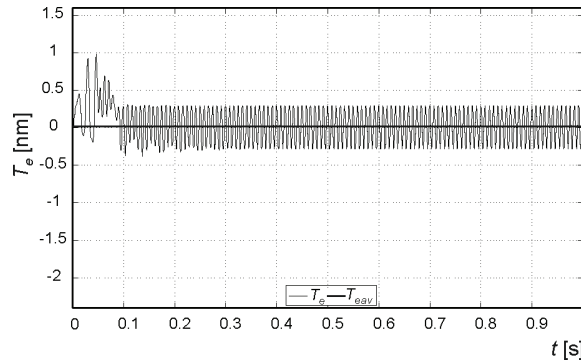
Fig. 4. The electromagnetic torque $T_e(t)$ at no-load for $C = 3\ \mu F$, $f = 60$ Hz
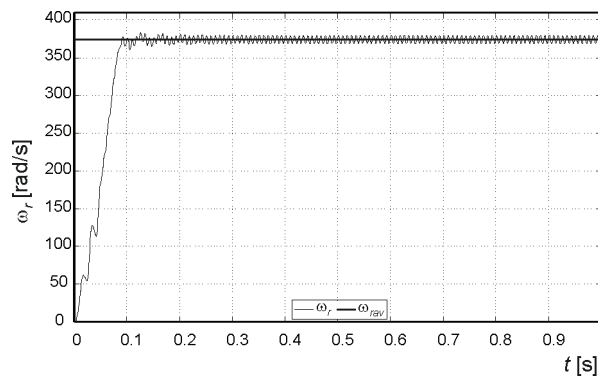

Fig. 5. The angular velocity $\omega_r(t)$ at no-load for $C = 3\ \mu F$, $f = 60$ Hz

which is the result of asymmetry of the stator windings and also different amplitudes of stator winding currents.

Torque oscillations influence directly speed's waveform, producing speed fluctuations. When the motor is supplied with voltage of frequency 60 Hz, the motor's magnetic field rotates with synchronous speed about 377 rad/s.
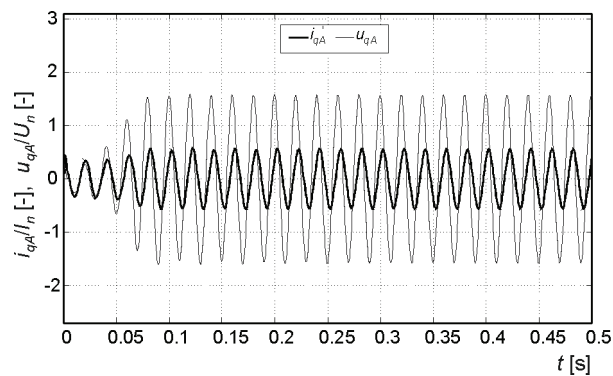
Fig. 6. The current and the voltage of stator auxiliary winding at no-load for $C = 3\ \mu F$, $f = 50$ Hz

This is the cause of the increase of the no-load speed, compared to 50 Hz. As might be expected, the amplitudes of torque and angular velocity oscillations are slightly lower at line frequency of 60 Hz. It is because amplitudes of both phase currents have more similar values. Line frequency influences phase shift between winding currents, too. Phase difference between currents and voltages of the auxiliary stator winding for no load and $C = 3$ µF at line frequency of 50 and 60 Hz is illustrated in Figures 6-7.
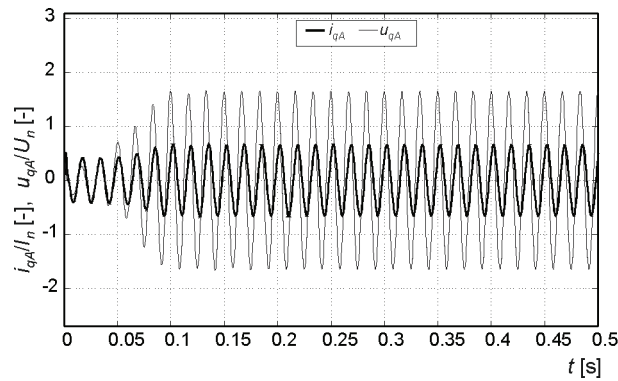
Fig. 7. The current and the voltage of stator auxiliary winding at no-load for $C = 3$ µF, $f = 60$ Hz

The waveforms for free-acceleration of the motor followed by application of rated load torque are shown in Figures 8-15.
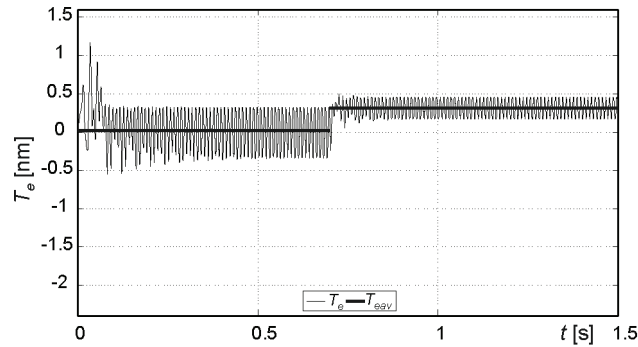
Fig. 8. The electromagnetic torque $T_e(t)$ at rated load for $C = 3$ µF, $f = 50$ Hz

After application of rated load torque, a decrease by 50% in the amplitude of electromagnetic torque and angular velocity is noticeable. This is because at the rated load, with properly chosen capacitance of a running capacitor, a rotating magnetic field in the air gap is more similar to the rotating circular field, which allows to obtain optimum conditions for stable operation at rated operating point.
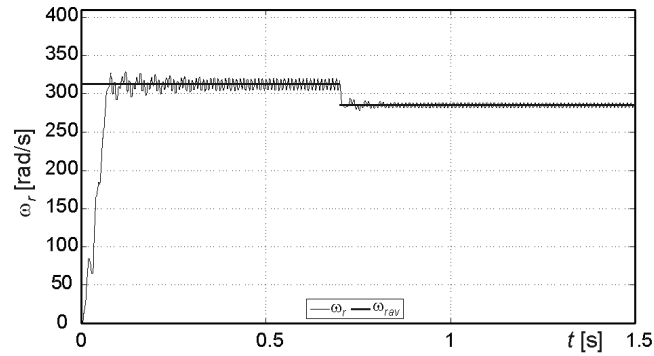
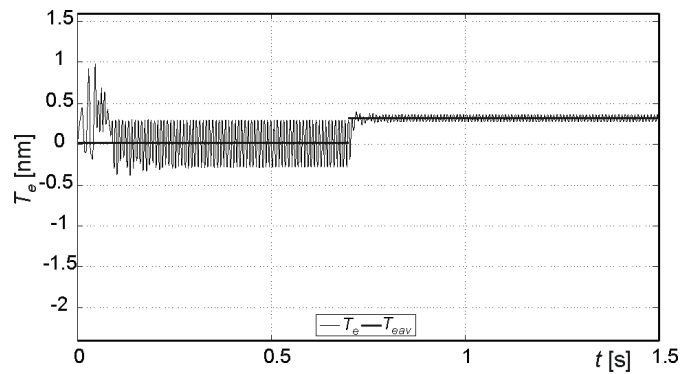Fig. 9. The angular velocity $\omega_r(t)$ at rated load for C = 3 µF, f = 50 Hz

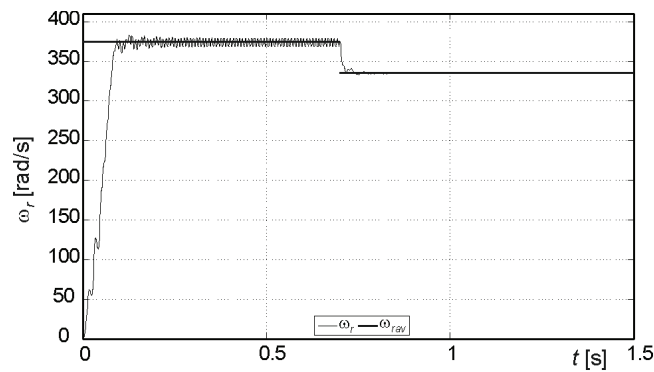Fig. 10. The electromagnetic torque $T_e(t)$ at rated load for C = 3 µF, f = 60 Hz

Fig. 11. The angular velocity $\omega_r(t)$ at rated load for C = 3 µF, f = 60 Hz

An influence of the running capacitor capacitance and line frequency on the electromagnetic torque, start-up time and pulsation of rotor velocity are shown in Figures 12-19.
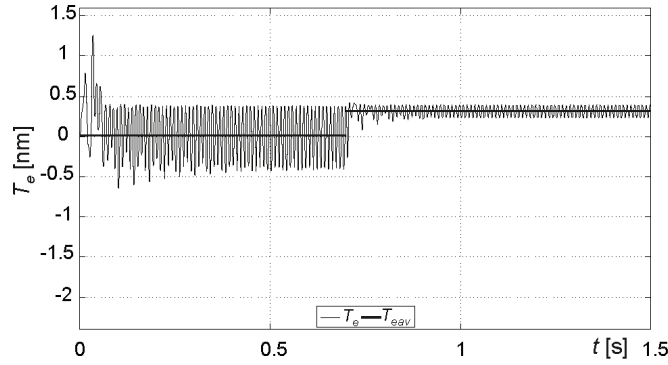
Fig. 12. The electromagnetic torque $T_e(t)$ at rated load for $C = 4$ µF, $f = 50$ Hz

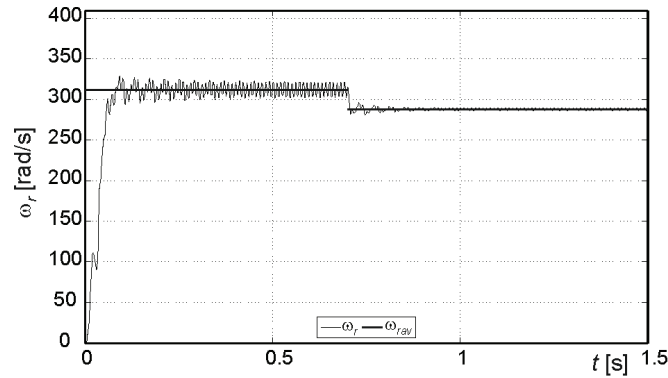Fig. 13. The angular velocity $\omega_r(t)$ at rated load for $C = 4$ µF, $f = 50$ Hz
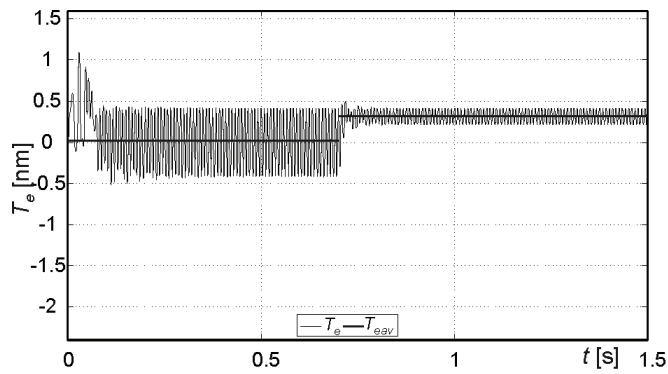

Fig. 14. The electromagnetic torque $T_e(t)$ at rated load for $C = 4$ µF, $f = 60$ Hz

It can be noticed that increasing running capacitor capacitance up to 4 µF decreases amplitude of electromagnetic torque's oscillations and slightly increases start-up time of the motor, when the motor is supplied with a voltage at frequency of 50 Hz. It gives better working conditions for the tested motor, as far as dynamic operation is concerned, because the
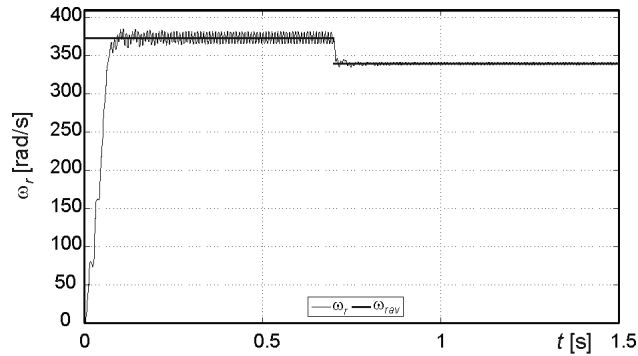
Fig. 15. The angular velocity $\omega_r(t)$ at rated load for $C = 4$ µF, $f = 60$ Hz
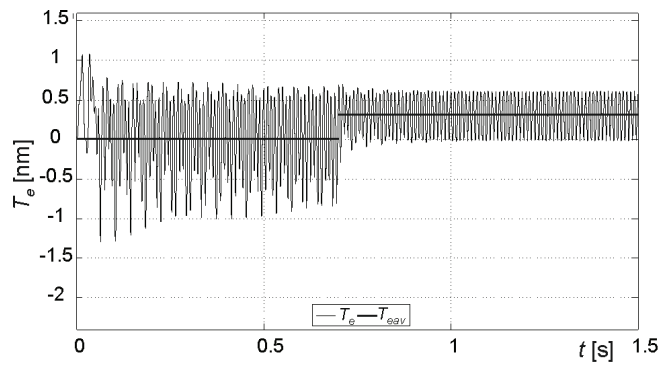
Fig. 16. The electromagnetic torque $T_e(t)$ at rated load for $C = 6$ µF, $f = 50$ Hz
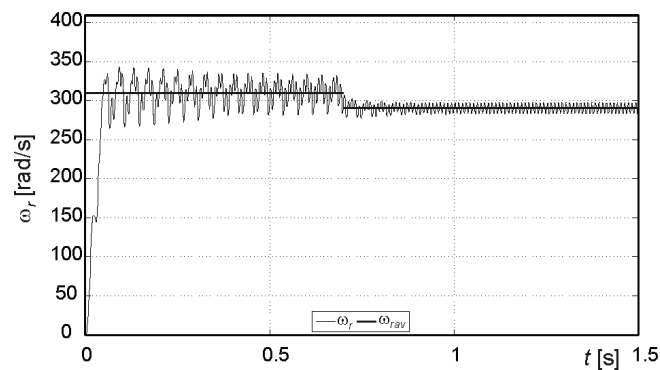
Fig. 17. The angular velocity $\omega_r(t)$ at rated load for $C = 6$ µF, $f = 50$ Hz

oscillations of the angular velocity are virtually eliminated. For $C = 4$ µF, amplitudes of phase currents have similar amplitudes and the rotating magnetic field in motor's air gap resembles circular magnetic field more closely. However, for the line frequency of 60 Hz, the amplitude
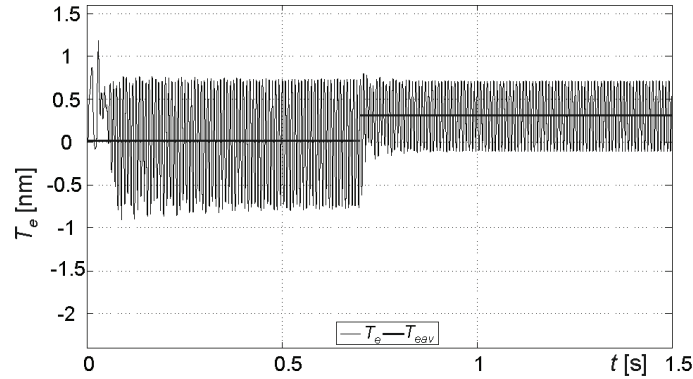
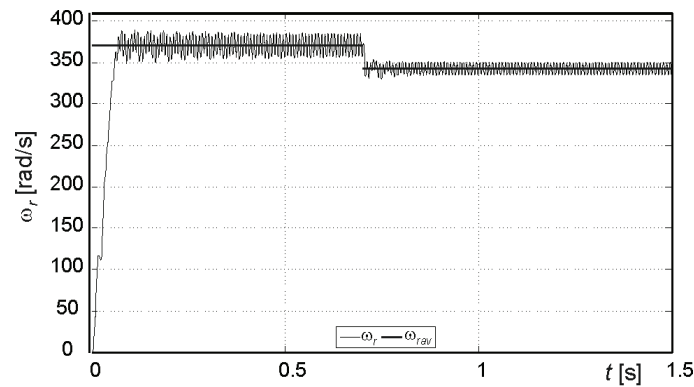Fig. 18. The electromagnetic torque $T_e(t)$ at rated load for $C = 6$ µF, $f = 60$ Hz

Fig. 19. The angular velocity $\omega_r(t)$ at rated load for $C = 6$ µF, $f = 60$ Hz

of aforementioned oscillations increases, compared to 3 µF – the rotating magnetic field is less similar to the circular field. Of course, the capacitor capacitance and line frequency influence on the phase difference between the main and auxiliary windings currents and also on the amplitudes of these currents.

Further increasing of the capacitance results in increase of amplitude of the electromagnetic torque oscillations, and consequently, also amplitude of angular velocity oscillations rises. It's because the rotating magnetic field is even less circular. Apart from oscillations, the motor operates with a strongly elliptical field will be also producing very loud noise. The start-up time for this case is also not to be reduced. For the tested motor, optimum conditions for stable operation (the lowest pulsations of torque and angular velocity) and the shortest start-up time may be obtained for the running capacitor capacitance in the range of 3-4 µF, regardless of the supply voltage frequency.

5. Steady-state characteristics of the motor

The steady-state operation of the capacitor induction motor was studied for different capacitor capacitance placed in the stator auxiliary winding and for two different line frequencies: 50 and 60 Hz. Computed electromagnetic torque and stator current versus relative rotational speed characteristics are shown in Figures 20-23.
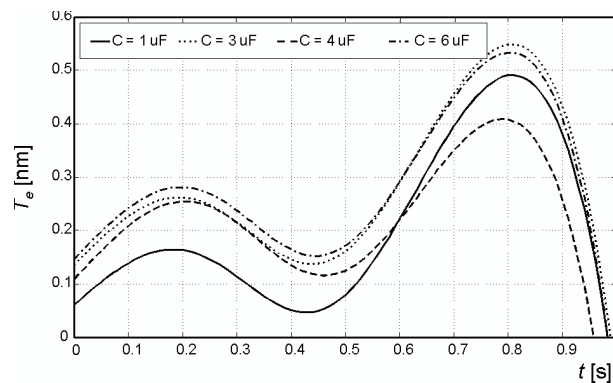

Fig. 20. Torque versus rotational speed characteristics for different capacitor capacitances and f = 50 Hz

Values of starting torques and starting and rated currents of the motor computed for different capacitor capacitances and line frequencies are listed in Tables 2 and 3. On the basis of these results, a starting quality factor, defined as a ratio of relative values of staring torque and starting current was evaluated and placed in the tables.

Table 2. Values of starting torques and starting and rated currents of the motor for different capacitor capacitances at the line frequency of 50 Hz

Capacitor capacitance [µF]	Starting torque [Nm]	Relative starting torque	Starting current [A]	Rated current [A]	Relative starting current	Starting quality factor
1	0.06	0.20	1.62	0.73	2.22	0.09
3	0.14	0.45	1.77	0.81	2.19	0.21
4	0.15	0.49	1.85	0.94	1.97	0.25
6	0.11	0.36	2.01	1.41	1.42	0.25

Table 3. Values of starting torques and starting and rated currents of the motor for different capacitor capacitances at the line frequency of 60 Hz

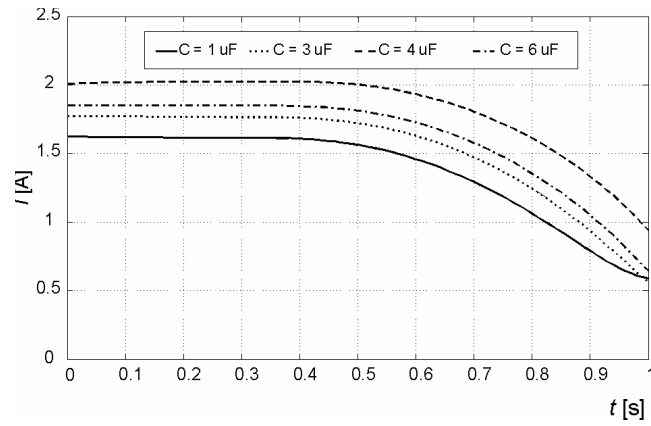| Capacitor capacitance [µF]	Starting torque [Nm]	Relative starting torque	Starting current [A]	Rated current [A]	Relative starting current	Starting quality factor
1	0.06	0.22	1.56	0.68	2.29	0.10
3	0.13	0.44	1.77	0.92	1.92	0.23
4	0.13	0.43	1.87	1.18	1.58	0.27
6	0.04	0.15	2.06	–	–	–

Fig. 21. Stator current versus rotational speed characteristics for different capacitor capacitances and f = 50 Hz
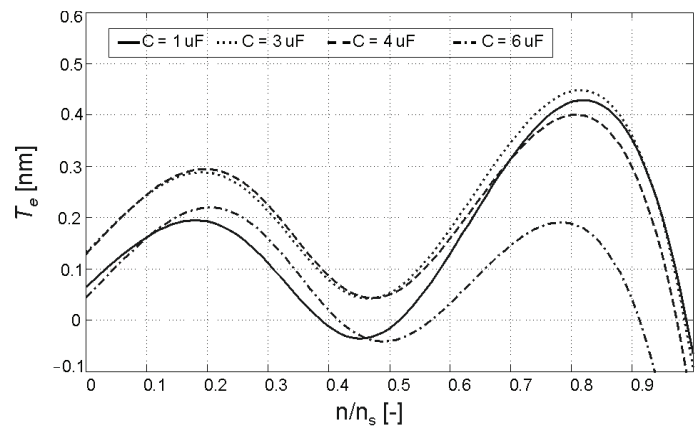

Fig. 22. Torque versus rotational speed characteristics for different capacitor capacitances and f = 60 Hz
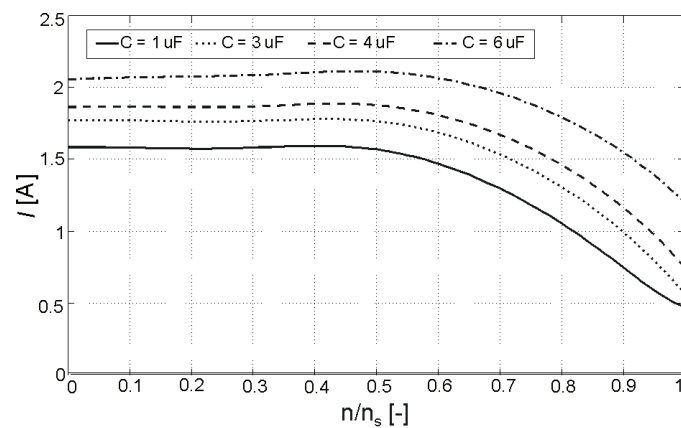

Fig. 23. Stator current versus rotational speed characteristics for different capacitor capacitances and f = 60 Hz

The torque-speed characteristics of capacitor induction motor exhibits a noticeable pull-up torque. It is caused by higher harmonics of the motor's magnetic field, especially by the third harmonic component. The parasitic torques may disrupt the process of starting, especially when the motor is loaded during start-up. The running capacitor's capacitance greatly influences the mechanical characteristic. For the line frequency of 50 Hz, capacity of 4 µF gives the best results. The capacitor capacitance of 3 µF also yields good results. For other capacitances, the parasitic torques generated by higher order harmonic components rise, which causes distortion of the torque-speed characteristics. For 60 Hz and for capacities of 1 µF and 6 µF, the pull-up torque is even less than zero.

The highest value of the starting torque amounts 0.15 Nm, which is obtained for the capacitor capacitance of 4 µF, regardless of the line frequency. For the capacitance selected by the motor's manufacturer (C = 3 µF), the result is only slightly worse (0.14 Nm). Any increase or decrease of the capacitance leads to decrease of the starting torque. Starting capacitor capacitance also affects the value of the motor's breakdown torque. It is significantly lower, when the motor is supplied with voltage of 60 Hz frequency. It should be mentioned, that the tested motor was designed to work with line frequency of 50 Hz.

The manufacturers selected the running capacitor's capacity with the aim of obtaining the circular rotating magnetic field in the motor's magnetic circuit, when the motor is loaded with rated load torque. It improves the rigidity of the torque-speed characteristic, and also increases the breakdown torque. For the running capacitor's capacitances other than 3 µF and 4 µF, the breakdown torque has smaller values and the motor's characteristic is less rigid. For C = 6 µF, the value of no-load speed also decreases. It is caused by the rotating elliptical magnetic field, that generates high-value backward (braking) component of the electromagnetic torque. When the motor is supplied with voltage of frequency 60 Hz, the breakdown torque decreases noticeable in comparison with the results for the frequency of 50 Hz. The running capacitor's capacitance of 6 µF again yields the worst results – the breakdown torque value – 0.22 Nm – is even smaller than the motor's rated torque T_N = 0.3 Nm.

For 50 Hz, the starting quality factor has the highest value for the capacitor capacitances of 4 and 6 µF. It may be misleading, because the absolute (irrelative) value of starting torque and starting current are respectively smaller and higher for 6 µF than for 4 µF. Similar results were obtained for the frequency of 60 Hz. The starting quality factor for 6 µF cannot be evaluated since the motor is unable to develop the rated torque of 0.3 Nm.

6. Conclusion

The paper presents the dynamic behavior and steady-state characteristics of the single-phase capacitor induction motor, supplied with voltage of frequency of 50 and 60 Hz, for different capacitances of the running capacitor.

The best operating conditions for the tested motor, as far as the dynamic operations are concerned, can be obtained for the running capacitor capacitance within the range of 3 ÷ 4 µF, for the line frequency of both 50 and 60 Hz – pulsations of the electromagnetic torque and the

angular velocity have then the minimal value. Steady-state performance parameters, like starting torque, starting current, pull-up torque and breakdown torque also have the most optimal values for the capacitance from the above mentioned range. The starting quality factor may be used as an additional factor for optimization and design of a single-phase induction motor since the starting torque and the starting current are very important parameters of the induction motors, especially when frequent direct-on-line starting is required. The presented mathematical model of the single-phase capacitor induction motor may be used as an efficient mathematical tool for prediction of performance characteristics of the motor already before its manufacturing.

References

[1] Yeadon W.H., Yeadon A.W., *Handbook of small electric motors.* McGraw-Hill (2001).
[2] Chapman S.J., *Electric Machinery Fundamentals.* McGraw-Hill, 4th ed. (2005).
[3] Lyshevski S.E., *Electromechanical Systems.* Electric machines and Applied Mechatronics, CRC Press (1999).
[4] Domijan A., Yin Y., *Single phase induction machine simulation using the electromagnetic transients program: Theory and test cases.* IEEE Trans. On Energy Conversion 9(3) September (1994).
[5] Faiz J., Ojaghi M., Keyhani A., *PSPICE simulation of single-phase induction motors.* IEEE Trans. On Energy Conversion 14(1) March (1999).
[6] Stankovic A.M., Lesieutre B.C., Aydin T., *Modeling and analysis of single-phase induction machines with dynamic phasors.* IEEE Trans. On Power Systems 14(1), February (1999).
[7] Makowski K., Wilk M., *Simulation of dynamic and steady-state operation of the single phase capacitor induction motor.* Electrical Review 85(10): 24-28 (2009).
[8] Makowski K., Wilk M.J., *Determination of dynamic characteristics of the single-phase capacitor induction motor.* Electrical Review 87(5): 231-237 (2011).
[9] Makowski K., *An analytical model and parameters of the single-phase capacitor induction motor, Modelling.* Simulation and Control, A, AMSE Press 21(2): 29-38 (1989).
[10] Śliwiński T., *Computational methods of induction motors.* (In Polish), PWN, Warsaw (2008).